Sputter Etching Rate Ratio of Si to SiO_2 using Mesh-Replica Method

Kadena Mogi*, Toshiya Ogiwara, Mineharu Suzuki, and SERD project of SASJ

NTT Advanced Technology Corporation, 3-1 Morinosato-Wakamiya, Atsugi, Kanagawa 243-0124, Japan

*E-MAIL: mogi@atsugi.ntt-at.co.jp

(Received: October 11, 2002; accepted November 5, 2002)

In depth profiling measurements with AES, XPS, and SIMS, the sputter etching rate is one of the important parameters. We have proposed the mesh-replica method (J. Surf. Anal. 5, 188 (1999)) to measure the actual sputtered depth even for a wide sputtered area. SERD (Sputter etching rate database) project in SASJ has been developing the relative sputter etching rate database using this technique. In this report, we show the sputter etching rate ratios of Si to SiO_2 by collaborating study, and they were determined to be 1.04±0.10 and 1.02±0.07 for the Ar^+ ion beam energies of 1 keV and 3 keV, respectively. From the results, it was found that the sputter etching rates of Si were almost the same as those of SiO_2.

1. Introduction

Depth profiling measurements with ion sputter etching is usually carried out in AES (Auger electron spectroscopy), XPS (X-ray photoelectron spectroscopy), and SIMS (secondary ion mass spectrometry). The sputter etching rate is one of the important parameters. Sputtering yields have been summarized from experimental data [1] and they are shown with the Z (atomic number) dependence. In their data, the sputtering yields increase with increasing the Z number, for example from Ti (Z=22) to Cu (Z=29), from Nb (Z=41) to Ag (Z=47), and so on. On the other hand, the U-valley shaped sputter etching rates are also shown in the literature [2]. For example, the sputter etching rates decrease from K (Z=19) to V (Z=23), are almost constant from V to Ni (Z=28), and increase from Ni to Se (Z=34). The same tendency are reported for Na (Z=11) to S (Z=16), Rb (Z=37) to Te (Z=52), and Cs (Z=55) to Tl (Z=81) for Ar ion bombardment. The numerical data for sputtering yields are listed for 17 kinds of single elemental metals in the reference [1]. These data are important to estimate a sputtered depth, however, it is difficult to judge the accuracy. This is because we experimentally know that sputter etching rates are different for crystallographic qualities (single crystal, poly-crystal, or amorphous) even for a same material, or for fabrication methods (sputter deposition, flatting, etc.). In AES and XPS, the sputter etching rate is generally estimated from an elemental depth profile of a standard sample with a known thickness such as a Ta_2O_5 film [3] or SiO_2 film [4]. The concept of relative sputter etching rate was previously introduced, and they were reported for sputter-deposited metal films normalized by the sputter etching rate of SiO_2 [5]. This method is useful in routine depth profiling measurements for various materials, then many data should be collected as a database for practical use. It is also important that the relative sputter etching rate is independent of ion current, ion current density, rastered area, and so on.

We have proposed the mesh-replica method to measure the actual sputtered depth [6]. In this report, we show the sputter etching rates of SiO_2 and Si mea-

This paper was presented at the International Symposium on Pratical Surface Analysis (PSA-01), 2001 in Nara, Japan.

Table 1 List of apparatus, ion gun type, and stylus profilometer used in the organizations.

Organization	Apparatus (AES, XPS)	Ion Gun type	Stylus profilometer
A	PHI-660 (AES)	Model 04-303	DEKTAK3030
B	PHI-680 (AES)	Model 06-350	DEKTAK3030
C	PHI Quantum 2000 (XPS)	----------	Surfcom900A
D	PHI-670 (AES)	Model 04-303A	DEKTAK2A
E	PHI-650 (AES)	FIG-5	DEKTAK3
F	PHI-670 (AES)	FIG-5	DEKTAK3030
G	PHI-660 (AES)	Model 04-303	DEKTAK3030

sured using mesh-replica method by collaborating seven organizations in SERD (Sputter etching rate database) project of SASJ (Surface Analysis Society of Japan). We have obtained the sputter etching rate ratios of Si to SiO_2 from these results.

A SiO_2 film is most familiar as a reference material with the depth marker, though it may be degraded by beam irradiation. On the other hand, the characteristics, such as crystallographic index and its purity, of Si substrate is well-defined and very stable against beam irradiation. Then we are considering that Si may become a candidate of a good reference material for sputtering rate when using the mesh-replica method.

2. Experimental

The specimens used were 100 nm-thick SiO_2 film and Si(100) substrate and sputtering processes were carried out by the AES apparatus (PHI, Model-650, 660, 670, and 680) and the XPS apparatus (PHI, Quantum 2000), as shown in table 1, with monitoring of elemental distribution in depth. The SiO_2 film was thermally grown on a Si(100) substrate and the thickness was determined by ellipsometry in our laboratory. Table 1 also shows the types of stylus profilometers used in this study. The ion for sputtering was Ar^+ with the energy of 1 keV or 3 keV and the incident angle of the ion beam were 59 degrees (PHI, Model-650, 660, and 670), 47 degrees (PHI, Model-680) and 45 degrees (PHI, Quantum 2000) from the surface normal. The sputter etching rates were varied by changing the rastered area of the ion beam and the ion sputtering was stopped before reaching the SiO_2 / Si interface for the SiO_2 films. The sputter etching rate of SiO_2 was measured by two methods: one is from the mesh-replica method and the other is from the depth profiling method. The latter one is to determine the sputter etching rate from the sputtering time from the top surface to the SiO_2 / Si-substrate interface. The sputter etch-

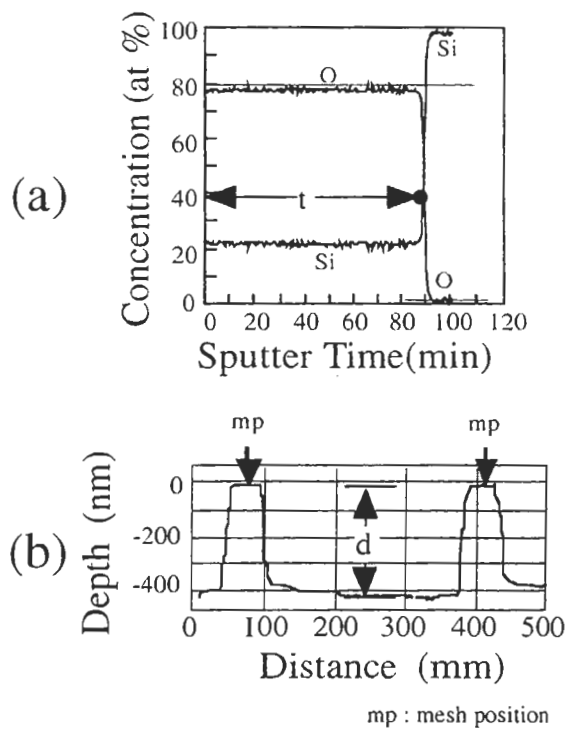

Fig. 1 (a) Example of depth profile of 100 nm-thick SiO_2 film. Thickness (100 nm) is *d* and sputtering time is *t*. (b) Example of stylus profilometer image after sputtering. Depth of sputtered crater is *d* and sputtering time is *t*.

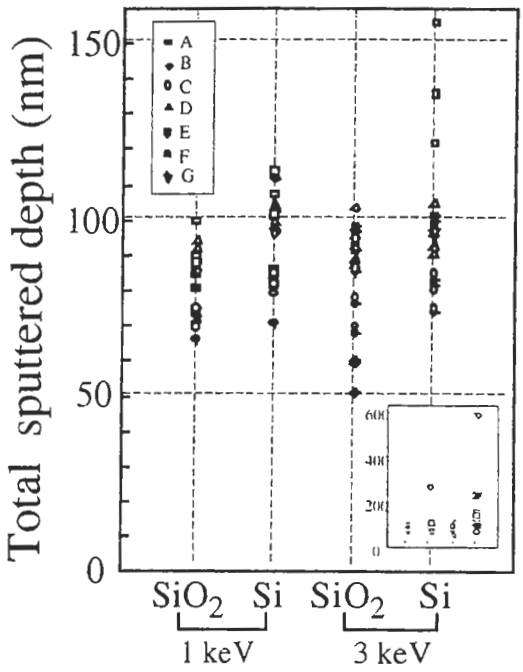

Fig. 2 Total sputtered depth of SiO_2 and Si for the Ar^+ ion beam energy of 1 keV and 3 keV. The organizations correspond to the symbols of A to G.

ing rate of Si was measured only by the mesh-replica method because of the lack of the depth-marking such as a compositional interface.

Figures 1 (a) and (b) show examples of a depth profile of 100 nm-thick SiO_2 film and a stylus profilometer image after sputtering. Using these data, sputter etching rates of SiO_2 were measured by the mesh-replica method and the depth profiling method.

3. Results and Discussion

3.1 Reported data from the collaborating organizations

Figure 2 show total sputtered depth of SiO_2 and Si for the Ar^+ ion beam energy of 1 keV and 3 keV in the seven organizations. The organizations correspond to the symbols of A to G. Total sputtered depth was measured using stylus profilometers. The inset graph includes all data, and the main graph expands the vertical axis because the measured values are almost distributed in the sputtered depth range below 160 nm. It is found that the measured values concentrate in the range of 60 to 110 nm.

Figures 3 (a) - (g) and (h) - (n) show the sputter etching rates of SiO_2 for the Ar^+ ion beam energy of 1 keV and 3 keV. Here, *NRD* for the horizontal axis is the abbreviation of *N*ominal X, Y *R*astering *D*istance for the sputtering, and *SER* for the vertical axis is for *S*putter *E*tching *R*ate. The horizontal axis corresponds to the reciprocal of the nominal rastering area. The unit of *NRD* is mm, then the unit of the horizontal axis is mm^{-2}.The sputter etching rate of SiO_2 was obtained by the depth profiling method (cf. Fig. 1(a)). Figures 4 (a) - (g) and (h) - (n) show the sputter etching rate of SiO_2 for the Ar^+ ion beam energy of 1 keV and 3 keV. The sputter etching rate of SiO_2 was obtained by the mesh-replica method (cf. Fig. 1(b)). The sputter etching rates of SiO_2 show the same linear-tendency against the reciprocal of NRD^2 values for almost all organization. At the NRD value of 2 ($1/NRD^2 = 0.25\ mm^{-2}$) in Figs. 3 (g) and 4 (g), however, the sputter etching rate at the organization G is larger, comparing those values obtained at other organizations.

Figures 5 (a) - (g) and (h) - (n) show the sputter etching rates of Si for the Ar^+ ion beam energy of 1 keV and 3 keV. The sputter etching rates of Si also show the similar curve. At the NRD value of 3 for the organization G in Fig. 5 (n), the sputter etching rate seems to be larger than other organizations. From Figs. 3 to 5, it means we should pay attention to the data at the organization G.

3.2 Sputter etching rate ratios depending on the ion beam raster area

Figures 6 (a) - (g) show the sputter etching rate ratio of Si to SiO_2 for the Ar^+ ion beam energy of 1 keV and 3 keV. The sputter etching rate of SiO_2 was obtained by the depth profiling method, and that of Si was obtained by the mesh-replica method. Figures 7 (a) - (g) show the sputter etching rate ratio of Si to SiO_2 for the Ar^+ ion beam energy of 1 keV and 3 keV. Here the sputter etching rates of SiO_2 and Si are obtained by the mesh-replica method. Figures 6 (g) - 2 and 7 (g) - 2 reduce the scale of the vertical axis of

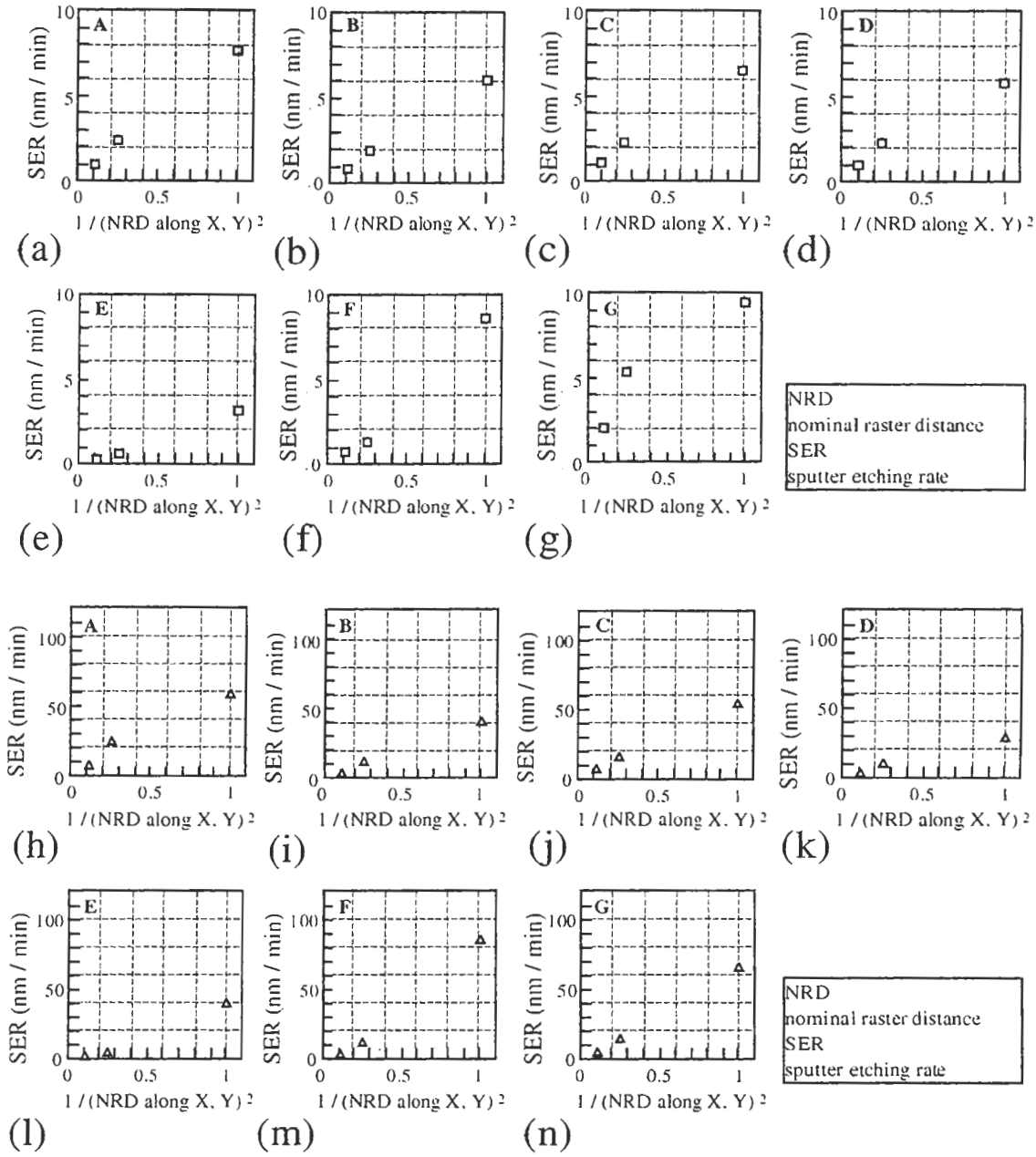

Fig. 3 (a) - (g): Sputter etching rate of SiO_2 for the Ar^+ ion beam energy of 1 keV. The sputter etching rate of SiO_2 is obtained by the depth profiling method. NRD and SER are the abbreviations of nominal X, Y rastering distance and sputter etching rate, respectively. Figures (a) to (g) correspond to the organization A to G.
(h) - (n): Sputter etching rate of SiO_2 for the Ar^+ ion beam energy of 3 keV. The sputter etching rate of SiO_2 is obtained by the depth profiling method. Figures (h) to (n) correspond to the organization A to G.
The unit of the horizontal axis in (a) - (n) is mm^{-2}.

Fig. 6 (g) - 1 and 7 (g) - 1, respectively. Since the value of the organization G of 3keV at the NRD of 3 ($1/NRD^2 = 0.11$ mm^{-2}) is particularly greater than other data in Fig. 6 (g) - 1, 6 (g) - 2, 7(g) - 1 and 7 (g) - 2, those two data were excepted in the following discussion.

The data in Fig. 6 (a) - (g) and Fig. 7 (a) - (g) are plotted in one figure as Fig. 8 and Fig. 9, respectively. The sputter etching rate ratios of Si to SiO_2 which obtained from the sputter etching rate of SiO_2 measured by the depth profiling method in Fig. 8 are widely spread in the range of 0.9-1.3. On the other hand, those

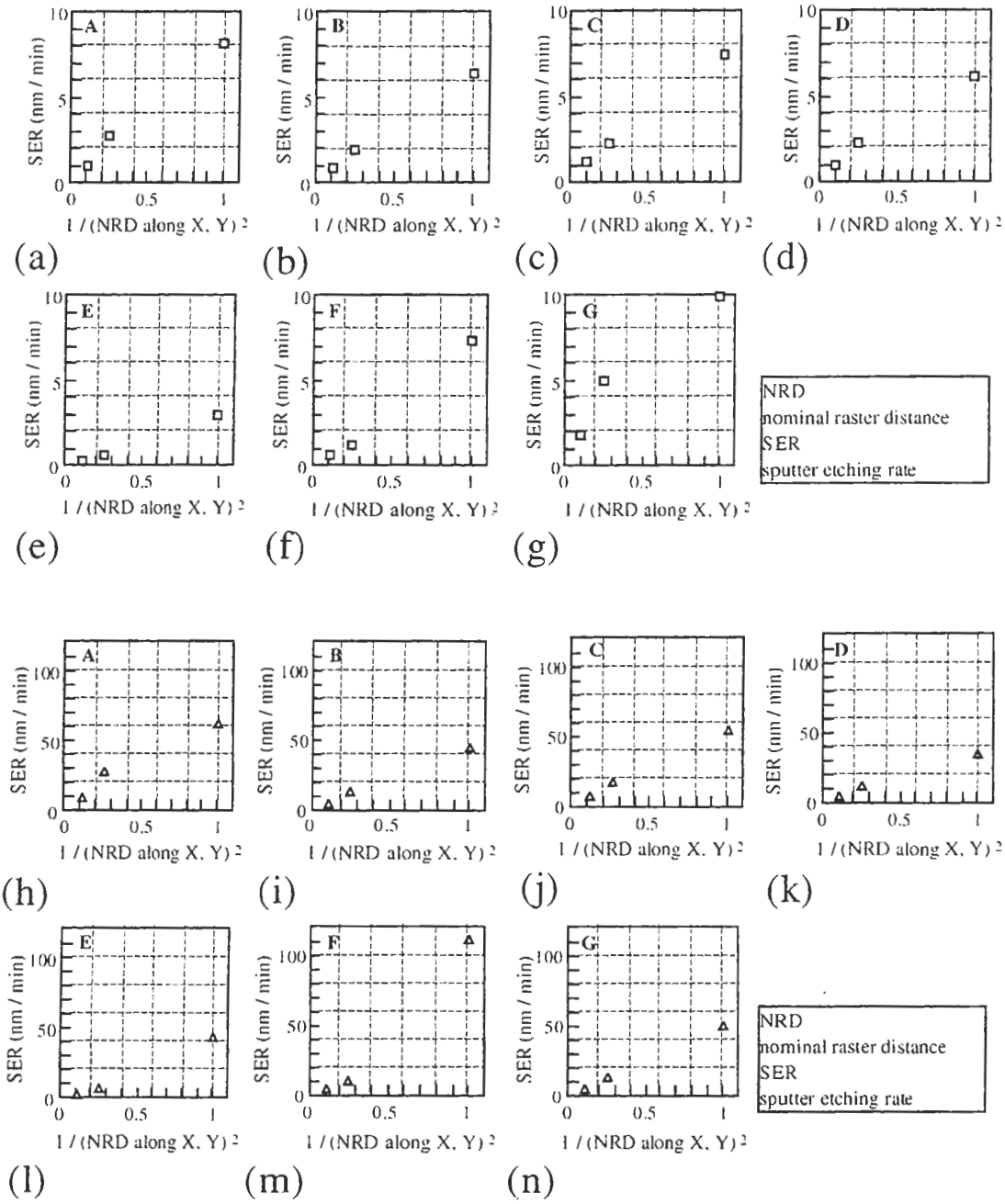

Fig. 4 (a) - (g): Sputter etching rate of SiO_2 for the Ar^+ ion beam energy of 1 keV. The sputter etching rate of SiO_2 is obtained by the mesh-replica method. Figures (a) to (g) correspond to the organization A to G.
(h) - (n): Sputter etching rate of SiO_2 for the Ar^+ ion beam energy of 3 keV. The sputter etching rate of SiO_2 is obtained by the mesh-replica method. Figures (h) to (n) correspond to the organization A to G.
The unit of the horizontal axis in (a) - (n) is mm^{-2}.

of Si to SiO_2 which obtained from the sputter etching rate of SiO_2 measured by the mesh-replica method in Fig. 9 are closely distributed, excepting the value of near 0.8 at NRD of 1 ($1/NRD^2 = 1\ mm^{-2}$) in Fig.9.

3.3 Correlation of Si and SiO_2 sputtering rates

Figures 10 (a) and (b) show the correlation of the sputter etching rates of Si with those of SiO_2 for the energies of 1 keV and 3 keV for the primary Ar^+ ion beam. The sputter etching rate of SiO_2 was obtained by the depth profiling method, and that of Si was obtained by the mesh-replica method. The sputter etching rate ratios of Si to SiO_2 were determined to be 1.05±0.16 and 1.11±0.07 for the Ar^+ ion beam ener-

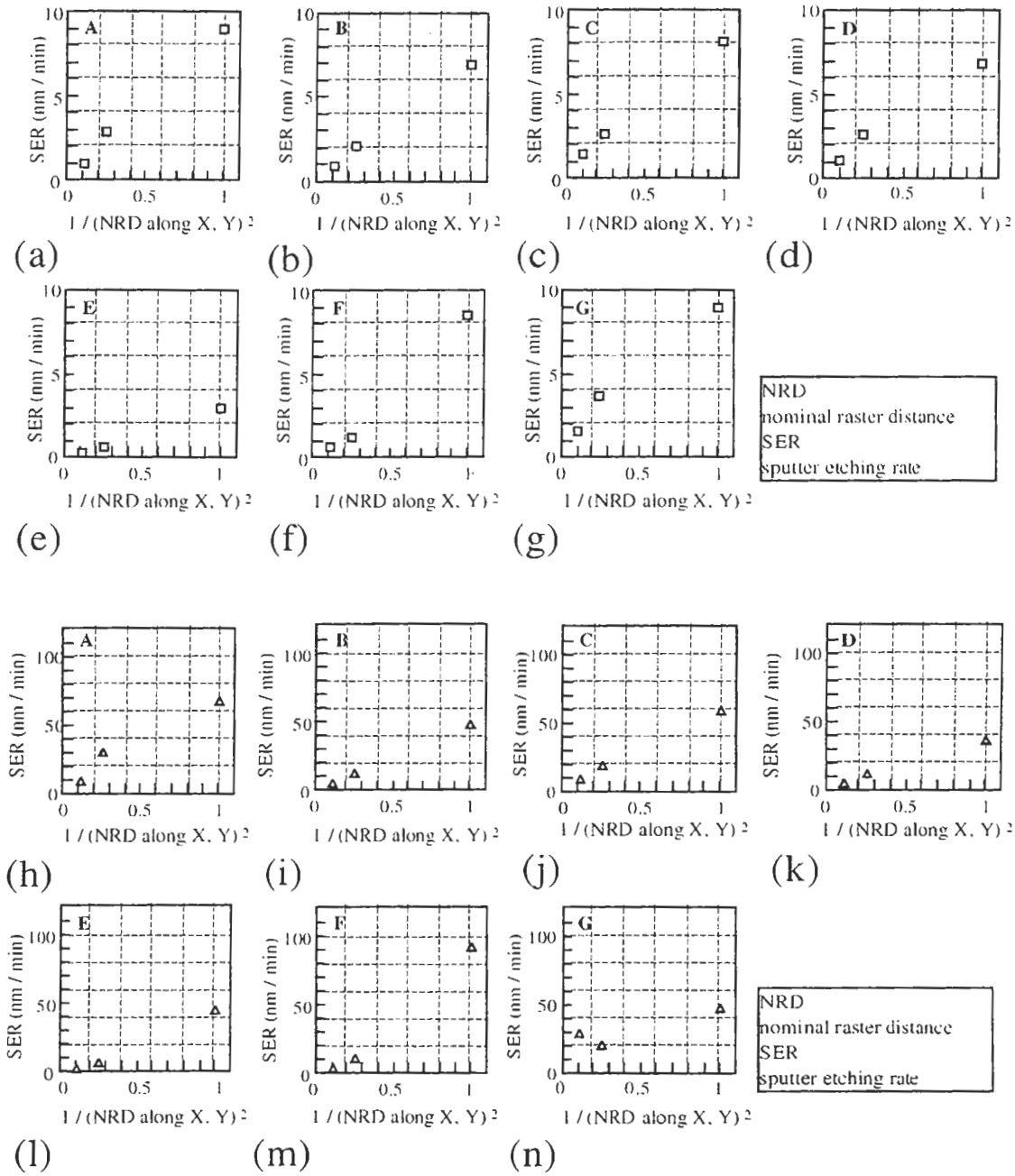

Fig. 5 (a) - (g): Sputter etching rate of Si for the Ar^+ ion beam energy of 1 keV. The sputter etching rate of Si is obtained by the mesh-replica method. Figures (a) to (g) correspond to the organization A to G.
(h) - (n): Sputter etching rate of Si for the Ar^+ ion beam energy of 1 keV. The sputter etching rate of Si is obtained by the mesh-replica method. Figures (n) to (n) correspond to the organization A to G.
The unit of the horizontal axis in (a) - (n) is mm^{-2}.

gies of 1 keV and 3 keV, respectively. Figures 11 (a) and (b) also show the correlation of the sputter etching rates of Si with those of SiO_2 for the energies of 1 keV and 3 keV for the primary Ar^+ ion beam. The sputter etching rates of SiO_2 and Si were obtained by the mesh-replica method. The sputter etching rate ratios of Si to SiO_2 were determined to be 1.04±0.10 and 1.02±0.07 for the Ar^+ ion beam energies of 1 keV and 3 keV, respectively. It is needed to examine the reproducibility of the sputter etching rate for an organization in order to precisely discuss, because it was not investigated in this study.

It is clearly found that the relative sputtering rates of Si to SiO_2 are linearly plotted independent of appa-

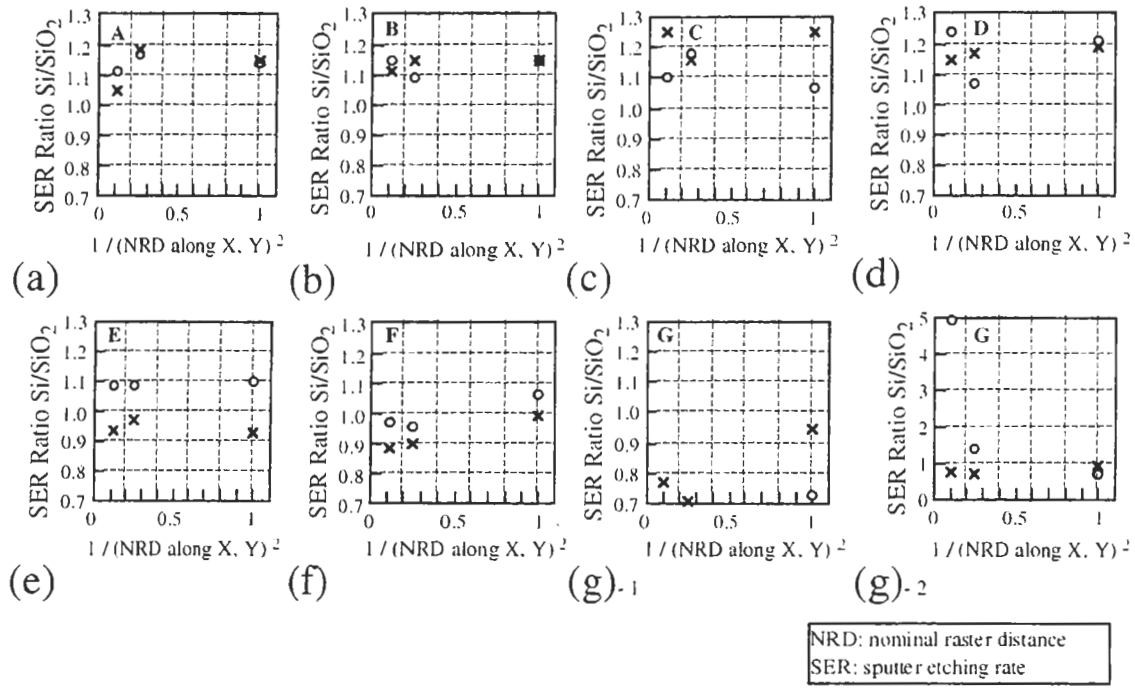

Fig. 6 (a) - (g): Sputter etching rate ratio of Si to SiO_2 for the Ar^+ ion beam energy of 1 keV (symbol X) and 3 keV (symbol O). The sputter etching rate of SiO_2 is obtained by the depth profiling method. The sputter etching rate of Si is obtained by the mesh-replica method. Figures (a) to (g) correspond to the organization A to G. Here, NRD and SER in axes correspond to nominal rastering distance and sputter etching rate, respectively. The unit of the horizontal axis in (a) - (g) is mm^{-2}.

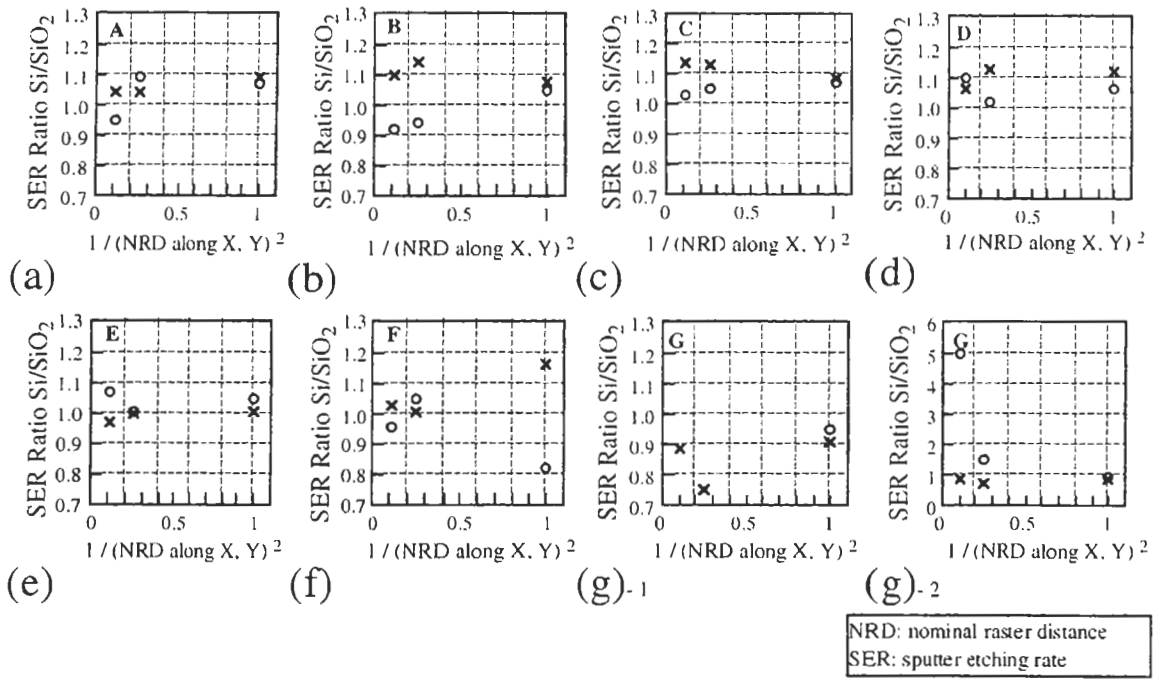

Fig. 7 (a) - (g): Sputter etching rate ratio of Si to SiO_2 for the Ar+ ion beam energy of 1 keV (symbol X) and 3 keV (symbol O). The sputter etching rate of SiO_2 and Si are obtained by the mesh-replica method. Figures (a) to (g) correspond to the organization A to G. Here, NRD and SER in axes correspond to nominal rastering distance and sputter etching rate, respectively. The unit of the horizontal axis in (a) - (g) is mm^{-2}.

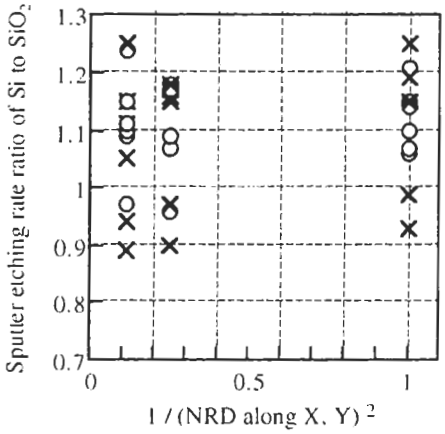

Fig. 8 Sputter etching rate ratio of Si to SiO_2 for the Ar^+ ion beam energy of 1 keV and 3keV. The sputter etching rate of SiO_2 is obtained by the depth profiling method. The sputter etching rate of Si is obtained by the mesh-replica method. The unit of the horizontal axis is mm^{-2}.

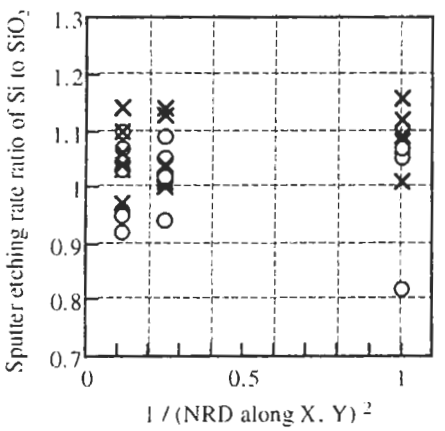

Fig. 9 Sputter etching rate ratio of Si to SiO_2 for the Ar^+ ion beam energy of 1 keV and 3keV. The sputter etching rates of Si and SiO_2 are obtained by the mesh-replica method. The unit of the horizontal axis is mm^{-2}.

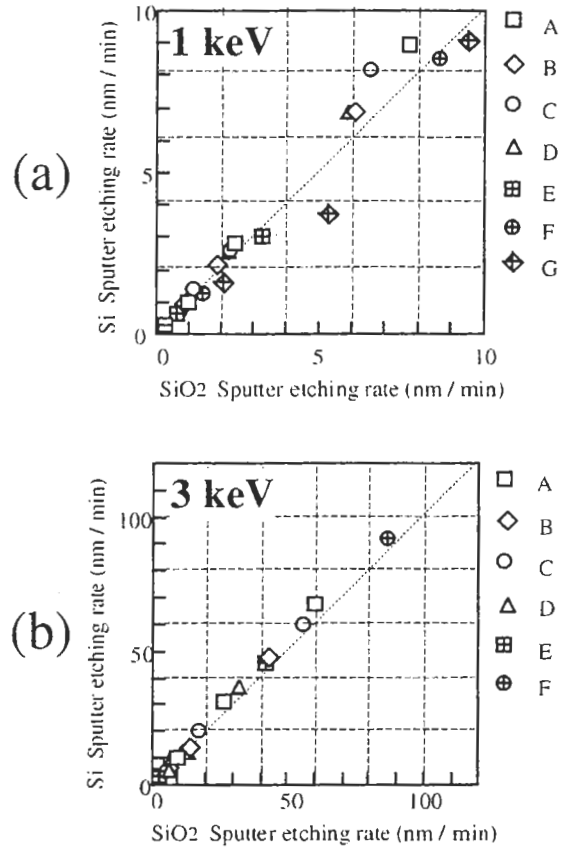

Fig. 10 Sputter etching rate of Si against that of SiO_2 for the Ar^+ ion beam energy of (a) 1 keV and (b) 3 keV. The sputter etching rate of SiO_2 is obtained by the depth profiling method. The sputter etching rate of Si is obtained by the mesh-replica method. The symbols A to G correspond to the organizations.

ratus and sputtering conditions, and that the sputter etching rates of Si were almost the same as those of SiO_2. It is also shown that the sputter etching rate ratios of Si to SiO_2 obtained from the depth profile method are slightly larger than those of Si to SiO_2 obtained from the mesh-replica method. This means that the sputter etching rate of SiO_2 which obtained by the depth profiling method is smaller than that of SiO_2 which obtained by the mesh-replica method. In Figs. 10 and 11, the dispersion of the sputter etching rate ratio is lager for the Ar^+ ion beam energy of 1 keV rather than that of 3 keV. In addition, the values for the organization G are particularly apart from a correlation line in Fig. 11 (a) and the point obtained by the organization F in Fig. 11 (b). We are considering that the problem may be in ion gun or stylus profilometer, though it is impossible to conclude the reason. Moreover, we think that the sputter etching rate is independent of the incident angle of the ion beams from 45 to 59 degrees in this study, considering the data in Figs. 10 and 11 do not depend on the apparatus type.

Figures 12 and 13 show normalized sputter etching rate, as unity at the NRD of 3 ($1/NRD^2$ = 0.11 mm^{-2}) from Figs.10 and 11, of Si and SiO_2 for the Ar^+ ion beam energy of 1 keV and 3 keV. When the value

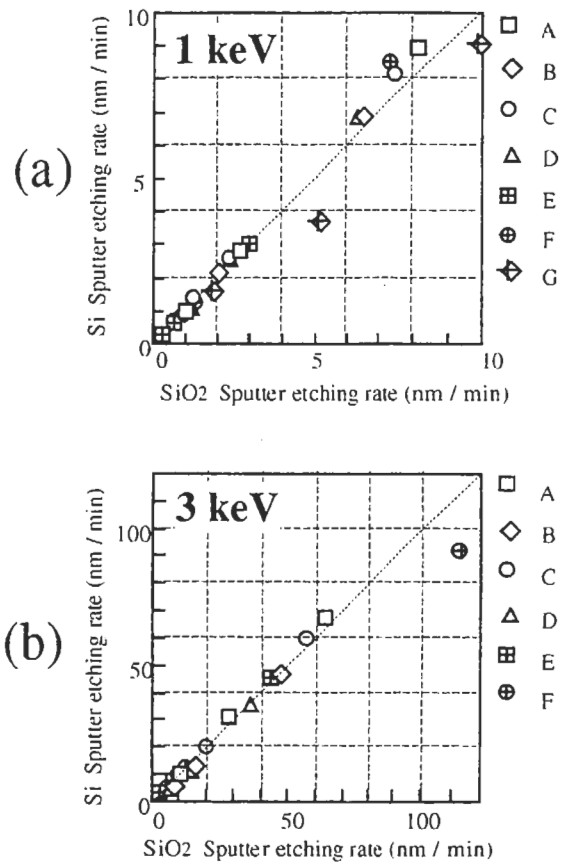

Fig. 11 Sputter etching rate of Si against that of SiO_2 for the Ar^+ ion beam energy of (a) 1 keV and (b) 3 keV. The sputter etching rates of Si and SiO_2 are obtained by the mesh-replica method. The symbols A to G correspond to the organizations.

of NRD is 1 ($1/NRD^2 = 1\ mm^{-2}$), the sputter etching rates of the organizations A, B, C and D are clearly smaller than those of the organization E and F. These two cathegories of the organizations use different ion gun as shown in Table 1, and it is thought that the characteristic of ion gun are shown.

4. Summary

We examined the sputter etching rate ratios of Si to SiO_2, which were obtained by mesh-replica method as well as by the depth profiling method. The experiments were carried out by seven organizations in SERD project in SASJ. The sputter etching rate ratios of Si to SiO_2 were determined to be 1.05±0.16 and 1.11±0.07 for the Ar^+ ion beam energies of 1 keV and 3 keV, respectively, from the sputter etching rate of

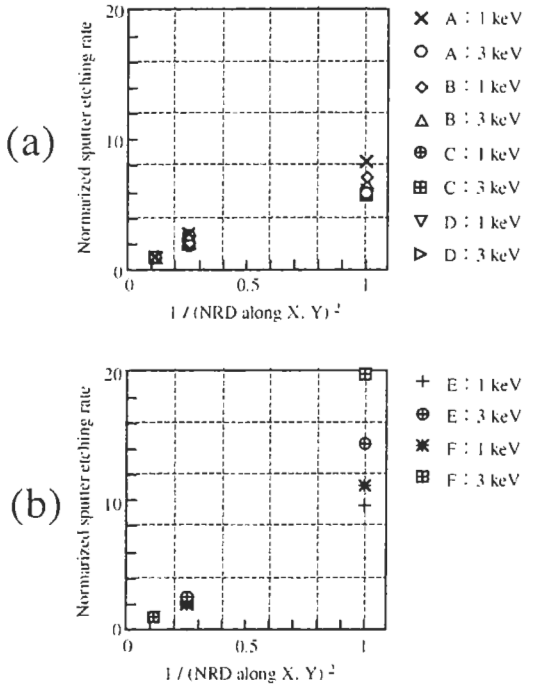

Fig. 12 (a), (b) Normalized sputter etching rate of SiO_2 for the Ar^+ ion beam energy of 1 keV and 3 keV. The sputter etching rate of SiO_2 was obtained by the depth profiling method.The unit of the horizontal axis is mm^{-2}.

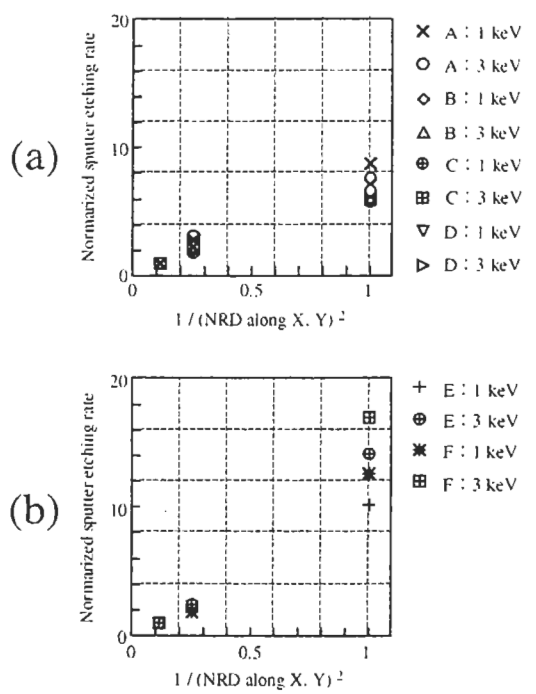

Fig. 13 (a), (b) Normalized sputter etching rate of SiO_2 for the Ar^+ ion beam energy of 1 keV and 3 keV. The sputter etching rate of SiO_2 was obtained by the mesh-replica method. The unit of the horizontal axis is mm^{-2}.

SiO_2 obtained by the depth profiling method. Those were determined to be 1.04±0.10 and 1.02±0.07 for the Ar^+ ion beam energies of 1 keV and 3 keV, respectively, from the sputter etching rate of SiO_2 obtained by the mesh-replica method. In both cases, the sputter etching rate of Si was obtained by the mesh-replica method.

From the results, it is found that the sputter etching rate of Si is almost equal to that of SiO_2. It is also shown that the sputter etching rate ratio of Si to SiO_2 obtained from the depth profile method is slightly larger than that of Si to SiO_2 obtained from the mesh-replica method, and we need further investigation to clarify the difference among these two methods. Moreover, the current study also shows the instrumental characteristics for the ion guns. If the additional experiments will be carried out using various types of ion guns, we are expecting that the detailed information is acquired.

Acknowledgement

This study was collaborated with Mr. R. Shinya (Sumitomo Metal Technology, Inc.), Mr. Y. Yamauchi (National Institute for Materials Science), Ms. N. Ishizu (Matsushita Techno-research, Inc.), Dr. Y. Ohtsuka (ULVAC, Inc.), Mr. S. Kakehashi (Mitsubishi Materials, Co.), and Mr. M. Nakamura (Fujitsu, Ltd.).

References

[1] H. W. Werner and P. R. Boudwijn, Chap. 5 "Depth Profiling Using Sputtering Methods" in "Beam Effects, Surface Topography, and Depth Profiling in Surface Analysis" ed. by A. W. Czanderna, T. E. Madey, and C. J. Powell, Plenum Press (1998). Data are cited from J. Appl. Phys. **32**, 365 8 (1961) by N. Laegrid and G. K. Wehner.

[2] H. J. Mathieu, chap. 4 "Auger Electron spectroscopy" in "Surface Analysis - The Principle Techniques" ed. by J. C. Vickerman, John Wiley & Sons (1997).

[3] BCR (Community Bureau of Reference, Belgium) CRM #261 Ta2O5 (32.2 / 97.0 nm) / Ta.

[4] NIST (National Institute of Standards and Technology) SRM #2531 to 2536 SiO2 (10 - 200 nm) / Si.

[5] N. Veisfeld and J. D. Geller, J. Vac. Sci. Technol., **A6**, 2077 (1988).

[6] M. Suzuki, K. Mogi, and H. Ando, J. Surf. Anal. **5**, 188 (1999).